Available online at www.sciencedirect.com
ScienceDirect
Chaos, Solitons and Fractals 39 (2009) 895–909
CHAOS
SOLITONS & FRACTALS
www.elsevier.com/locate/chaos

Ergodicity breakdown and scaling from single sequences

Armen K. Kalashyan [a], Marco Buiatti [b,c], Paolo Grigolini [a,d,e,*]

[a] Center for Nonlinear Science, University of North Texas, P.O. Box 311427, Denton, TX 76203-1427, USA
[b] Laboratoire de Neurophysique et Physiologie, CNRS UMR 8119 Université René Descartes – Paris 5 45, rue des Saints Pères, 75270 Paris Cedex 06, France
[c] Cognitive Neuroimaging Unit – INSERM U562, Service Hospitalier Frederic Joliot, CEA/DRM/DSV, 4 Place du general Leclerc, 91401 Orsay Cedex, France
[d] Dipartimento di Fisica "E.Fermi" – Università di Pisa and INFM, Largo Pontecorvo 3, 56127 Pisa, Italy
[e] Istituto dei Processi Chimico, Fisici del CNR Area della Ricerca di Pisa, Via G. Moruzzi 1, 56124 Pisa, Italy

Accepted 22 January 2007

Abstract

In the ergodic regime, several methods efficiently estimate the temporal scaling of time series characterized by long-range power-law correlations by converting them into diffusion processes. However, in the condition of ergodicity breakdown, the same methods give ambiguous results. We show that in such regime, two different scaling behaviors emerge depending on the age of the windows used for the estimation. We explain the ambiguity of the estimation methods by the different influence of the two scaling behaviors on each method. Our results suggest that aging drastically alters the scaling properties of non-ergodic processes.

1. Introduction

A very popular way to analyze time series rests on the Brownian motion (BM) paradigm. A time series $\{\xi_i\}$ is a sequence of values depending on the subscript i, which is interpreted as a form of discrete time, ranging from $i = 1$ to $i = L$, where L is a very large integer value. If L is very large, we can adopt the continuous time representation

$$x(t) = \int_0^t \xi(t')\,\mathrm{d}t', \tag{1}$$

with t being an integer number fulfilling the condition:

$$1 \ll t \ll L. \tag{2}$$

This means that the time series $\{\xi_i\}$ is thought of as being an one-dimensional diffusion generating fluctuation. When the BM condition applies, the fluctuation is random and has a finite variance. As a consequence, the width of the corresponding probability distribution density (pdf), $p(x,t)$, with x denoting the diffusion coordinate, increases as the

* Corresponding author. Tel.: +1 409 565 3294.
E-mail address: grigo@df.unipi.it (P. Grigolini).

0960-0779/$ - see front matter © 2007 Elsevier Ltd. All rights reserved.
doi:10.1016/j.chaos.2007.01.062

square root of time. A plausible conjecture for the time series generated by a complex system, of whatever nature, biological, sociological or geological, is that the time series depart significantly from this condition, insofar as they reflect the long-range cooperation among the constituents of the system under study. As a consequence, if these time series are adopted to generate diffusion, a significant departure from the Brownian motion diffusion would ensue.

A special attention is devoted to determining the asymptotic scaling of this diffusion process, which is defined by

$$p(x,t) = \frac{1}{t^{\delta_{\text{th}}}} Q\left(\frac{x}{t^{\delta_{\text{th}}}}\right), \tag{3}$$

with δ_{th} usually termed scaling coefficient, or scaling (the suffix 'th' stands for theoric to distinguish it from the scaling estimates δ that will be introduced shortly). The BM condition is represented by $\delta_{\text{th}} = 1/2$ and $Q(y)$ equal to a gaussian function of the argument y. In the literature a special attention is therefore being devoted to estimating the scaling δ_{th}. The most popular estimation methods based on diffusion are the standard deviation analysis (SDA) [3], the diffusion entropy analysis (DEA) [2] and the detrended fluctuation analysis (DFA) [1].

The SDA [3] rests on

$$D^2(l) \equiv \langle (\Delta x(l) - \langle \Delta x(l) \rangle_{l_0})^2 \rangle_{l_0}, \tag{4}$$

where l_0 is the initial point of the walk, the l_0 subscript on the bracket means an average on the initial position of the mobile window of size l and

$$\Delta x(l) \equiv x(l_0 + l) - x(l_0). \tag{5}$$

The initial position l_0 of the mobile windows of size l moves one step a time from $+0$ to $L - l$, so as to create as many Gibbs systems as possible using a single sequence. If fluctuations $\{\xi_i\}$ are not random but exhibit long-range power-law correlations, $D(l)$ scales as

$$\lim_{l\to\infty} D(l) \propto l^{\delta}, \tag{6}$$

where in the ergodic regime, $0.5 < \delta < 1$, and the relation between δ and δ_{th} generally depends on the nature of the underlying process [4]. The mobile window method used for the SDA is shared by the DEA. As in the case of SDA, the windows of the same length serve the purpose of creating diffusion trajectories moving from the origin at $l = 0$ and spreading with the increase of l. Rather than evaluating the standard deviation of this diffusion process, the DEA evaluates the entropy of the resulting distribution of walkers, usually the Shannon entropy, $S(l)$, thereby making the result independent of linear biases, with no need of adopting a preliminary de-trending, and directly estimating the scaling δ_{th} through the important property [2]

$$S(l) = A + \delta \log(l), \tag{7}$$

where A is a constant depending on the function $Q(y)$ of Eq. (3).

DFA technique [1] operates as follows. First of all the trajectory $x(t)$ of Eq. (1) is evaluated, with t ranging from $t = 0$ to $t = L$. The single sequence, of length L, is divided into $N \approx L/l$ non-overlapping windows. Thus the window label is given by $l_0 = ml$ with m ranging from $+0$ to $N - 1$. Within every window a linear fit $x_{\text{lin}}(t)$ to $x(t)$ is computed: The quantity $(x(t) - x_{\text{lin}}(t))^2$ fluctuates as t moves from $t = l_0$ to $t = l_0 + l$. The DFA measure is the mean value of these fluctuations. Finally, this measure is averaged over all l_0, yielding the square root mean residual of the fluctuations

$$F(l) = \sqrt{\left\langle \frac{1}{l} \sum_{l_0}^{l_0+l} (x(t) - x_{\text{lin}}(t))^2 \right\rangle_{l_0}}, \tag{8}$$

which is expected to hold:

$$\lim_{l\to\infty} F(l) \propto l^{\delta}. \tag{9}$$

with the same scaling δ given by the SDA (Eq. (6)) [1,6].

All three methods address the same main difficult problem and solve it in the same way. The problem to solve is the following. Statistical physics rests on the use of the Gibbs ensemble method, an important requirement that the time series analysis cannot meet. A single time series represents the time evolution of a single system, and in the case of physiological, geophysical and sociological processes, the Gibbs ensemble concept is an ideal condition that cannot be realized in practice, not even approximately. Each complex systems is unique, and an average on many identical systems cannot be done. Thus all three methods rest on the implicit assumption that the time series represents the time evolution of a system, whose complex rules do not change with time. Special refinements are necessary to cope with the difficult

case of changing with time rules [5]. In this article, we make the assumption that the rules driving the system's time evolution *do not change with time*. Thus, in principle, we might safely use the solution adopted by all three methods to bypass the problem caused by the lack a Gibbs ensemble. This is, in fact, the adoption of moving windows which rests on the tacit assumption of ergodicity.

The recent work of Refs. [7–9] shows that many physical systems generate time series that are not ergodic, even if the rules driving their dynamics do not change with time. Moreover, several biological time series exhibit a non-ergodic behavior [10–12], and the estimation of the temporal scaling is not supported by a clear theory as in the ergodic case.

In this paper, we plan to discuss the consequences that these non-ergodic properties have on the results of the SDA, DEA and DFA analysis. The common adoption of the moving window method is supplemented by different prescriptions, the detrending with DFA, and no detrending whatsoever with DEA. We plan to show that the ergodicity breakdown causes these different prescriptions to produce different scalings. To make this discussion easier we create a time series that has been widely studied in the past as a source of super-diffusion [4,13–15]. Following the authors of Ref. [13] we call this model *velocity model*. In the earlier work the statistical analysis of this time series has been done in a stationary condition generating Lévy walk [4,15]. Here we use the velocity model in the non-ergodic condition, where the scaling is age dependent.

We begin by showing with numerical simulations on single time series generated by the velocity model that SDA, DEA and DFA give ambiguous results in the non-ergodic regime. In the literature there already exist prescriptions to determine the scaling dependence on aging, thereby yielding a variety of scalings, ranging from the infinitely aged to the brand new condition. See, for instance, Refs. [16,17] for a recent discussion on the Gibbs approach to aging and aging dependent scaling. Assuming a Gibbs approach, we derive analytically and numerically the two scalings corresponding to the infinitely aged and the brand new condition of the velocity model in the non-ergodic regime. We show that, when analysing single sequences, the SDA is insensitive to the aged scaling predicted by the ordinary Gibbs ensemble method, while such scaling is predominant in the DFA. We show that the DEA does not afford a neat scaling, but only a slow transition to an undefined time asymptotic scaling that probably corresponds to the Gibbs aged condition.

2. Generation and scaling analysis of non-ergodic time series

It is easy to show [18] that the transformation

$$\tau = T\left(\frac{1}{y^{\frac{1}{\mu-1}}} - 1\right), \tag{10}$$

with $\mu > 1$, has the effect of turning the sequence $\{y_i\}$ of random numbers uniformly distributed in the interval $[0, 1]$ into the sequence $\{\tau_i\}$ with the probability density $\psi(\tau)$ given by

$$\psi(\tau) = (\mu - 1)\frac{T^{\mu-1}}{(\tau + T)^{\mu}}. \tag{11}$$

We use this prescription to generate the time sequence $\{t_i\}$ defined by

$$t_i = \tau_i, \tag{12}$$

if $i = 1$, and by

$$t_{i+1} = \tau_i + t_i, \tag{13}$$

if $i > 1$.

We are now in a position to define the velocity model of Ref. [13], which is a prescription to derive the time series $\{\xi\}$, with the following rule: The modulus of the fluctuation $\xi(t)$ is constant (and set for simplicity equal to $+1$). At the time t_i we toss a coin to establish the sign of the velocity for the whole interval $t_i \leqslant t < t_{i+1}$.

Note that the mean time $\langle\tau\rangle$ is given by

$$\langle\tau\rangle = \frac{T}{\mu - 2}. \tag{14}$$

When $\mu < 2$, the mean value $\langle\tau\rangle$ diverges and the time series $\{t_i\}$ is not ergodic [8,9]. The authors of Ref. [4] applied the DEA to the case $2\langle\mu\rangle 3$ and found that the DEA reveals the Lévy walk scaling

$$\delta = \frac{1}{(\mu - 1)}, \tag{15}$$

whereas the SDA, based on the long-time limit of the second moment,

$$\langle x^2(t)\rangle \propto t^{2\delta}, \tag{16}$$

yields

$$\delta = \frac{4-\mu}{2}. \tag{17}$$

The authors of Ref. [15] pointed out that the pdf $p(x,t)$ is a truncated Lévy distribution. If we ignore this truncation, the scaling δ of Eq. (15) is the proper scaling of Eq. (3). This Lévy distribution is truncated by two symmetric ballistic peaks whose scaling is $\delta = 1$. As a consequence this dynamic process is biscaling and SDA scaling is a compromise between the Lévy scaling of Eq. (15) and the faster peak ballistic scaling. Using these arguments the authors of Ref. [19] proved, by using DEA and SDA, that the model illustrated in this section is the proper representation of DNA sequences, thereby supporting the earlier work of [20].

No one of these earlier papers explored the non-ergodic region $\mu < 2$. It is only known, on the basis of theoretical arguments [13] that in this case the ballistic scaling

$$\delta = 1 \tag{18}$$

should apply.

Here we explore the transition from the ergodic to non-ergodic condition by means of SDA (Fig. 1), DEA (Fig. 2) and DFA (Fig. 3), using 5 different values of μ across the transition: $\mu = 1.6$, 1.8, 2.0, 2.2 and 2.4. We generated for each value of μ a single artificial sequence of length $L = 10^6$, and we assigned to T in Eq. (10) the value $T = 0.5$. For every sequence, we checked that the distribution density of Eq. (11) had the asymptotic power-law behavior predicted theoretically. SDA and DEA were computed by following the prescriptions described in the Introduction, i.e. with overlapping windows whose initial position are shifted one step at a time. DFA was computed with windows overlapping for half of their length. We checked with further simulations that the portion of window overlapping does not affect the DFA estimate; the half-window overlap was preferred to the almost complete overlap used for SDA and DEA to speed up computations.

For $\mu \geqslant 2$, this simulation confirms the well-known scaling $\delta = (4-\mu)/2$, Eq. (17), for SDA and DFA, and $\delta = 1/(\mu-1)$, Eq. (13) for DEA. For $\mu \leqslant 2$, three distinct behaviors emerge. As expected from [3,13], the SDA slope in log–log scale saturates to 1 (Figs. 1 and 4). The results produced by the DEA remain ambiguous since no clear scaling appears for time windows shorter than $t \simeq 15,000$ (Figs. 2 and 4).

It is remarkable that the DFA method does not perceive the transition from the ergodic to the non-ergodic condition, and obeys the prescription $\delta = (4-\mu)/2$ throughout Figs. 3 and 4. As a consequence, in the non-ergodic regime, the scaling emerging from the DFA exceeds the ballistic scaling $\delta = 1$. At first sight, this seems to be unphysical insofar as the walkers of velocity model move with constant velocity and consequently travel distances proportional to t. We shall see that this is a consequence of the ergodicity breakdown.

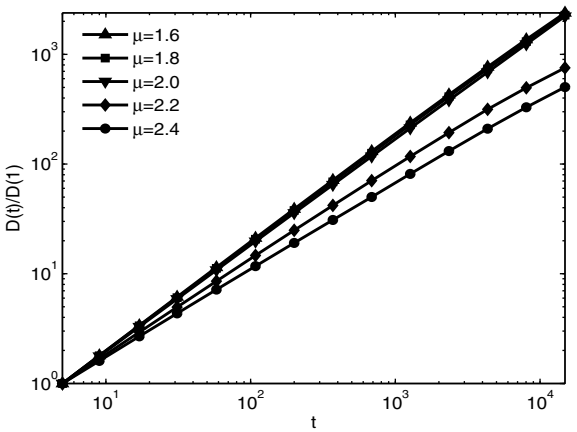

Fig. 1. SDA on the five artificial sequences with varying μ. Every curve shows $D(t)/D(1)$ in function of the diffusion time t in bilogarithmic scale. Correspondence between curves and values of μ is indicated in the legend on the top left of the figure.

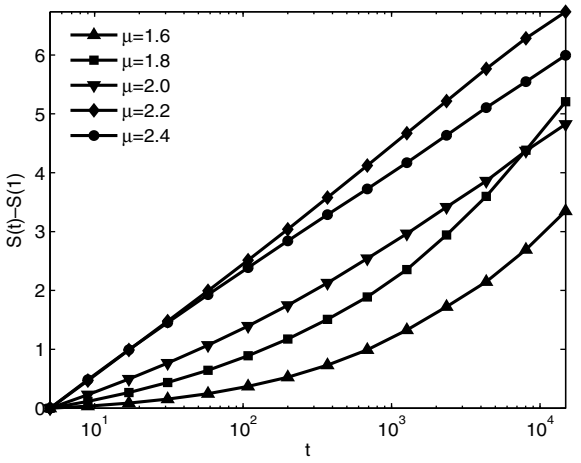

Fig. 2. DEA on the five artificial sequences with varying μ. Every curve shows $S(t) - S(1)$ in function of the diffusion time t in semilogarithmic scale. Correspondence between the curves and values of μ is indicated in the legend on the top left of the figure.

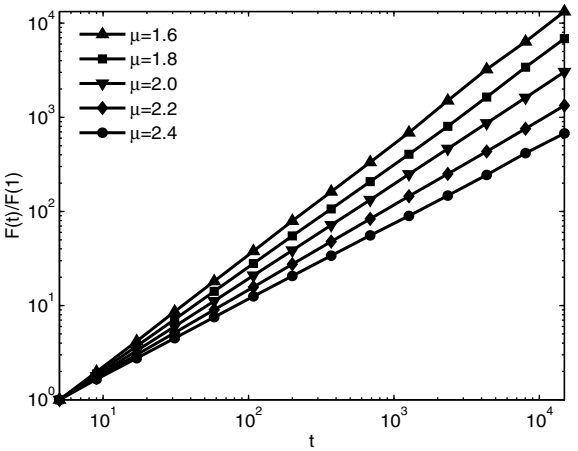

Fig. 3. DFA on the five artificial sequences with varying μ. Every curve shows $F(t)/F(1)$ in function of the diffusion time t in bilogarithmic scale. Correspondence between curves and values of μ is indicated in the legend on the top left of the figure.

3. Renewal aging

The time series $\{t_i\}$ used in Section 2 is renewal and non-exponential at the same time. An important property, directly related to $\psi(t)$, is the probability that no event occurs during a given time interval t. This quantity, called $\Psi(t)$, is given by

$$\Psi(t) = \int_t^{+\infty} \mathrm{d}t' \psi(t'). \tag{19}$$

The choice of Eq. (11) yields

$$\Psi(t) = \left(\frac{T}{t+T}\right)^{\mu-1}, \tag{20}$$

namely, a rate of event occurrence changing with time, thereby producing aging effects [16,21]. The functions $\psi(t)$ and $\Psi(t)$ depend on the time at which observation begins. Let us assume that the time series under study is prepared in such a way that the first event occurs at $t = 0$. The probability density of meeting an event at a later time t is given by $\psi(t)$ of Eq. (11) and the probability that no event occurs up to time t is given by $\Psi(t)$ of Eq. (20). If we begin the observation at

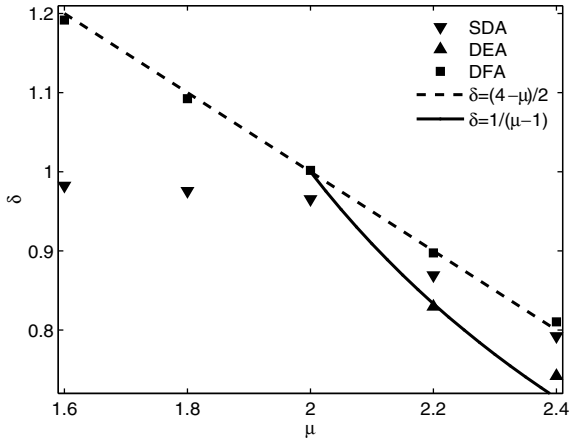

Fig. 4. Scaling exponents δ estimated by SDA, DEA and DFA in function of μ. The dashed line represents the theoretical prediction for SDA and DFA $\delta = (4-\mu)/2$, while the solid line represents the prediction for DEA $\delta = 1/(\mu-1)$. Only two points are plotted for DEA since for $\mu \leqslant 2.0$ no clear scaling appears.

a time $t' > 0$, the probability density of meeting an event is not more given by $\psi(t)$ of Eq. (11). Under the only condition that the time series is renewal, the probability density of meeting an event at time $t > t'$, given the condition that observation begins at t', denoted as $\psi(t,t')$, is given by [16]

$$\psi(t,t') = \sum_{n=0}^{\infty} \int_0^{t'} \mathrm{d}t'' \psi_n(t'')\psi(t-t''). \tag{21}$$

The function $\psi_n(t)$ is the probability density that at time t the last of a sequel of n events occurs. Due to the renewal character of the process $\psi_n(t)$ is related to $\psi_{n-1}(t)$ by

$$\psi_n(t) = \int_0^t \mathrm{d}t' \psi_{n-1}(t')\psi_1(t-t'), \tag{22}$$

with

$$\psi_1(t) \equiv \psi(t). \tag{23}$$

A much more practical expression for $\psi(t,t')$ is given by [16]

$$\psi(t,t') = \frac{\int_0^{t'} \psi(t+y)}{K_{t'}}\,\mathrm{d}y, \tag{24}$$

where $K_{t'} \equiv K(t') = \int_0^{t'} \Psi(t'')\,\mathrm{d}t''$ is the normalization constant. This expression is derived from Eq. (21) by assuming that the function

$$P(t) = \sum_{n=0}^{\infty} \psi_n(t) \tag{25}$$

is time independent.

Note that in addition to the delayed waiting time distribution $\psi(t,t')$ it is convenient to define the corresponding survival probability

$$\Psi(t,t') = \int_t^{\infty} \mathrm{d}y \psi(y,t'). \tag{26}$$

In conclusion, in the non-Poisson case, the explicit form of $\psi(t)$ depends on the time at which observation begins. The waiting time distribution of Eq. (11) might be denoted as $\psi(t,0)$, insofar as it corresponds to beginning the observation at the time itself at which an event occurs.

To explain how aging may influence scaling, let us review first the CTRW prescription generalized by Zumofen and Klafter [13] to determine the time evolution of $p(x,t)$ when preparation and observation occur at the same time. According to this prescription we have

$$p(x,t) = \Psi(x,t) + \sum_{n=1}^{\infty} \int_0^t \mathrm{d}t' \int_{-\infty}^{+\infty} \mathrm{d}x' \psi_n(x',t') \Psi(x-x', t-t'), \tag{27}$$

where $\psi_n(x,t)$ and $\Psi(x,t)$ have the following meaning. $\psi_n(x,t)$ is the probability density for the walker to move a distance x in time t as a result of n events, the last of which makes the walker arrive at x exactly at time t. Due to the renewal character of the process the function $\psi_n(x,t)$ is related to $\psi_{n-1}(x,t)$ through

$$\psi_n(x,t) = \int_0^t \mathrm{d}t' \int_{-\infty}^{\infty} \mathrm{d}x' \psi_{n-1}(x',t') \psi_1(x-x', t-t'). \tag{28}$$

The function $\Psi(x,t)$ is the probability for the walker to move a distance x with no event occurring up to time t.

The time and space convoluted nature of Eq. (27) makes it convenient to adopt the Fourier–Laplace transform method. The Fourier–Laplace transform of $p(x,t)$ is denoted by the symbol $\hat{p}(k,u)$, and after a little algebra, and summation of a geometric series, Eq. (27) becomes

$$\hat{p}(k,u) = \frac{1}{1-\hat{\psi}(k,u)} \hat{\Psi}(k,u). \tag{29}$$

The velocity model corresponds to setting

$$\psi(x,t) = \frac{1}{2}[\delta(x-t) + \delta(x+t)]\psi(t), \tag{30}$$

and

$$\Psi(x,t) = \frac{1}{2}[\delta(x-t) + \delta(x+t)]\Psi(t). \tag{31}$$

With Eq. (30) we select from the distribution density $\psi(t)$ a time t, throughout which the walker moves with constant velocity, in either the positive or the negative direction, according to a fair coin tossing prescription. Using Eq. (31) we take into account the motion of the random walkers before completion of the soujourn times in one of the two velocity states. As earlier pointed out, the scaling $\delta = 1$ seems to be the maximum possible scaling. In fact, the authors of Ref. [13] found the scaling of Eq. (15) for $2 < \mu < 3$ and the scaling of Eq. (18) for $1 < \mu < 2$. This is because they have used for all jump events the prescription of Eq. (30). This is correct if at $t = 0$ all the random walkers are found at the beginning of their velocity state. This condition corresponds to making observation and preparation occur at the same time.

To find the scaling dependence on aging, we properly prepare the Gibbs ensemble of time sequences at $t = 0$, by assuming that all of them at that time are at the beginning of a velocity state. Then we imagine that the corresponding walkers are located at $x = 0$ at a time $t' > 0$. Thus, the first event occurrence is described by

$$\psi(x,t,t') = \frac{1}{2}[\delta(x-t) + \delta(x+t)]\psi(t,t'), \tag{32}$$

with $\psi(t,t')$ given by Eq. (21), rather than by Eq. (30). On the same token, Eq. (31) is replaced by

$$\Psi(x,t,t') = \frac{1}{2}[\delta(x-t) + \delta(x+t)]\Psi(t,t'). \tag{33}$$

After the first event occurrence, we go back to using the ordinary functions $\psi(t)$ and $\Psi(t)$.

Applying this prescription to Eq. (27), we turn $p(x,t)$ into $p(x,t,t')$, namely a pdf corresponding to preparing the fluctuation $\xi(t)$ at $t = 0$ and the random walker leaving the origin $x = 0$ at time $t' > 0$. By evaluating the Laplace transform of Eq. (27) with the first event occurrence described by $\psi(t,t')$, by Fourier–Laplace transforming, and summing the geometric series, we obtain

$$\hat{p}(k,u,t') = \hat{\Psi}(k,u,t') + 2\pi\hat{\psi}_1(k,u;t')\hat{\Psi}(k,u)\frac{1}{1-\sqrt{2\pi}\hat{\psi}(k,u)}. \tag{34}$$

Note that in the Fourier space

$$\psi_1(k,\tau,t') = \frac{1}{\sqrt{2\pi}}\psi(\tau,t')\cos[k\tau], \tag{35}$$

$$\psi(k,\tau) = \frac{1}{\sqrt{2\pi}}\psi(\tau)\cos[k\tau] \tag{36}$$

and

$$\Psi(k,\tau)=\frac{1}{\sqrt{2\pi}}\cos[k\tau]\int_{\tau}^{+\infty}\psi(t')\,\mathrm{d}t'. \tag{37}$$

Rather than using the variables t and t' we deem to be more convenient to adopt the variables t' and $\tau\equiv t-t'$.

4. Delayed waiting time distribution

This section is devoted to the discussion of the waiting time distribution $\psi(t,t')$. According to Section 3, this function is essential to evaluate $p(x,t,t')$ and thus the dependence of scaling on t'. Moreover, as we shall see, this delayed waiting time distribution allows us to determine the scaling corresponding to the condition $\tau\ll t'$.

The exact expression of Eq. (21) is not convenient for a qualitative discussion of the aging process. A simple way to derive the main properties of $\psi(\tau,t')$ is given by Eq. (24), which yields

$$\psi(\tau,t')\simeq(\alpha-1)\frac{(\tau+T)^{-\alpha}-(\tau+T+t')^{-\alpha}}{T^{1-\alpha}-(t'+T)^{1-\alpha}}, \tag{38}$$

where

$$\alpha\equiv\mu-1. \tag{39}$$

Let us consider the following two limiting conditions: (a) $\tau\gg t'\gg T$; (b) $T\ll\tau\ll t'$. With two straightforward Taylor expansions for $1<\mu<2$, we obtain

$$\psi(\tau,t')\approx\frac{(2-\mu)(\mu-1)t'^{(\mu-1)}}{\tau^{\mu}} \tag{40}$$

and

$$\psi(\tau,t')\approx\frac{(2-\mu)t'^{(\mu-2)}}{\tau^{\mu-1}}, \tag{41}$$

respectively. This results allow to derive immediately the scaling corresponding to the conditions (a) and (b). In fact, the normalized the correlation function of the fluctuation $\xi(t)$, $\Phi_{\xi}(\tau,t')$ is known [17]. Its Laplace transform with respect to τ yields

$$\hat{\Phi}_{\xi}(u,t')=\frac{1-\frac{2\hat{\psi}(u,t')}{1+\hat{\psi}(u)}}{u}. \tag{42}$$

It is straightforward to prove that for $u\to 0$

$$\hat{\Phi}_{\xi}(u,t')\propto\hat{\Psi}(u,t'). \tag{43}$$

Thus, conditions (a) and (b) yield for $\tau\to\infty$

$$\Phi_{\xi}(\tau,t')\propto\tau^{1-\mu} \tag{44}$$

and

$$\Phi_{\xi}(\tau,t')\propto\tau^{2-\mu}, \tag{45}$$

respectively.

On the other hand, the evaluation of the second moment of $x(t)$ from Eq. (1) brings for $t\to\infty$

$$\langle x^2(t)\rangle=\langle\xi^2\rangle\int\int\mathrm{d}t'\,\mathrm{d}\tau\Phi_{\xi}(\tau,t'). \tag{46}$$

Let us make the conjecture that in this double integral the weight of the condition (b) is predominant. As a consequence for $\tau\to\infty$

$$\frac{\mathrm{d}^2}{\mathrm{d}t^2}\langle x^2(t)\rangle\propto t^{2-\mu}. \tag{47}$$

Thus, in condition (b), the scaling $\delta=(4-\mu)/2$ of the second moment typical of the ergodic regime persists in the non-ergodic regime. The paradoxical result of DFA of Section 2 is then explained in terms of the predominance of the aged condition (b).

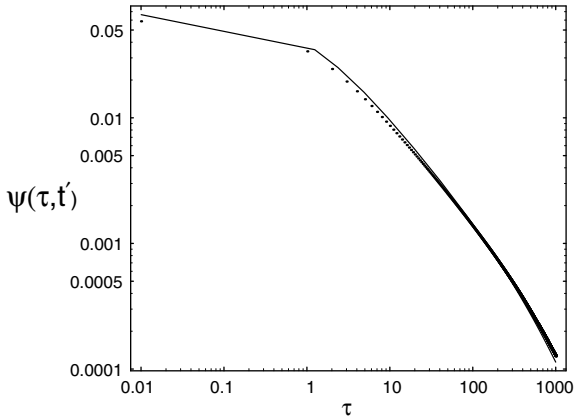

Fig. 5. The probability density function(PDF) for the first event times in log–log scale.The dots are obtained exactly anti-Laplace transforming analytical expression (48) with respect to second variable. The solid line is the plot of expression (38). The numerical constants are: $\mu = 1.8,\ t' = 10^3,\ T = 1$.

However, the arguments that we have used are based on the approximated expression of Eq. (38) that might be inaccurate in the non-ergodic case $\mu < 2$. For this reason we compare Eq. (38) to the exact prediction of Eq. (21). This is done as follows. We evaluate the Laplace transform of $\psi(\tau, t')$, and we use the symbol s to denote the variable that is the Laplace conjugate of t'. We obtain the following exact expression

$$\hat{\psi}(\tau, s) = \frac{e^{s\tau}}{1 - \hat{\psi}(s)} \left[\hat{\psi}(s) - \int_0^{\tau} e^{-s\zeta} \psi(\zeta)\, d\zeta \right], \tag{48}$$

where $\hat{\psi}(s) = \alpha e^{sT} [sT]^{\alpha} \Gamma[-\alpha, sT]$ is the Laplace transform of Eq. (11) and $\Gamma[a, z] = \int_z^{+\infty} t^{a-1} e^{-t}\, dt$ is the incomplete gamma function. The numerical-exact anti-Laplace transformation with respect to variable s is performed according to Talbot algorithm in the programing language Mathematica5.2. The graphical comparison between numerical-exact anti-Laplace transform with respect to s of Eq. (48) and approximated-analytical form Eq. (38) of $\psi(\tau, t')$ is shown in Fig. 5 for $\mu = 1.8$ and the agreement between approximated expression and exact prediction is remarkably good. The value of μ adopted for this comparison ($\mu = 1.8$) is close to the border $\mu = 2$. We expect that the approximated expression becomes less accurate as we move towards $\mu = 1$. However, the exact expression of Eq. (48) in the limiting conditions $t' \gg T$ and $\tau \gg T$ can be inverted analytically. It yields for $0 < \alpha < 1$

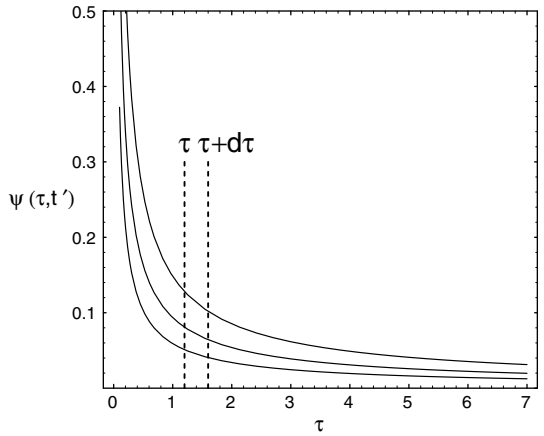

Fig. 6. For illustration purposes it is simply plotted the probability density function (PDF) for the first event times according to Eq. (50) for $T \ll \tau \ll t'$ in linear scale. The numerical constants are: $\mu = 1.8,\ T = 10^{-3},\ t' = 10^4,\ 10^5,\ 10^6$. Increasing t' the curves decay faster. $\psi(\tau, t')\, d\tau$ is the probability that the event will occur in the time interval $d\tau$ if we observe the system at t'.

$$\psi(\tau,t') \simeq \frac{\sin[\pi\alpha]}{\pi}\frac{t'^{\alpha}}{\tau^{\alpha}(\tau+t')}. \tag{49}$$

From this analytical expression it is straightforward to derive

$$\psi(\tau,t') \sim \begin{cases} \frac{t'^{(\mu-1)}}{\tau^{\mu}} & \text{for } T \ll t' \ll \tau, \\ \frac{t'^{(\mu-2)}}{\tau^{\mu-1}} & \text{for } T \ll \tau \ll t'. \end{cases} \tag{50}$$

By comparison with Eqs. (40) and (41), we see that, although the exact result significantly departs from the approximated expression of Eq. (24), the scalings of the conditions (a) and (b) are correct. In conclusion, this result offers an explanation of the paradoxical result of Section 2 about the DFA scaling estimate.

Before concluding this section, we want to shed further light into the aging effect by plotting $\psi(\tau,t')$ for increasing values of t'. We see from Fig. 6 that the larger t' the smaller the probability of event occurrence, and consequently the longer the sojourn time in one state. The system becomes slower, thereby justifying the term aging to denote this effect.

5. Second moment

We are now ready to evaluate the scaling $\delta(\tau,t')$. This is done defining

$$z \equiv \log\tau \tag{51}$$

and setting

$$\delta(\tau,t') = \delta(e^{z},t')|_{z=\log\tau} = (1/2)\left.\frac{\mathrm{d}[\log\langle x^2(e^{z},t')\rangle]}{\mathrm{d}z}\right|_{z=\log\tau}. \tag{52}$$

It is straightforward to prove that

$$\langle \hat{x}^2(u,t')\rangle = -\left.\frac{\partial^2\hat{p}(k,u;t')}{\partial k^2}\right|_{k=0} \tag{53}$$

By using Eqs. (34), (35), (36), (37) and (53) we derive after somewhat lengthy algebra the following simple expression

$$\langle \hat{x}^2(u,t')\rangle = \frac{\hat{\psi}(u,t')}{1-\hat{\psi}(u)}\left[\frac{\partial^2}{\partial u^2}\frac{1-\hat{\psi}(u)}{u} + \frac{1}{u}\frac{\partial^2\hat{\psi}(u)}{\partial u^2}\right]. \tag{54}$$

At this stage we benefit from the results of Section 4. We use Eq. (49) and the convolution theorem to get, in the limiting cases $\tau \gg T$ and $t' \gg T$

$$\langle x^2(\tau,t')\rangle \cong \frac{(1-\alpha)\sin[\pi\alpha]}{\pi(\alpha^2-3\alpha+2)}\frac{\tau^{1-\alpha}}{t'}[t'[(\alpha-3)\tau+(\alpha-2)t'] - (\alpha-2)(\tau+t')^2{}_2F_1\left(1,1-\alpha;2-\alpha;-\frac{\tau}{t'}\right)], \tag{55}$$

where ${}_2F_1$ is the hypergeometric function. Finally, using Eq. (52),

$$\delta(\tau,t') \cong \frac{(\alpha-2)\tau[-t' + {}_2F_1(1,1-\alpha;2-\alpha;-\frac{\tau}{t'})(\tau+t')]}{A(\tau,t')+B(\tau,t')}, \tag{56}$$

where

$$A(\tau,t') \equiv (\alpha-2){}_2F_1(1,1-\alpha;2-\alpha;-\frac{\tau}{t'})(\tau+t')^2 \tag{57}$$

and

$$B(\tau,t') \equiv t'(3\tau+2t'-\alpha(\tau+t')). \tag{58}$$

We illustrate Eq. (56) in Fig. 7. We see that upon increase of t' the transition from the scaling of Eq. (17) to the well known ballistic scaling becomes slower and slower, so as to make it virtually permanent in the case of infinitely large age. This sheds further light into the action of DFA. Finally, we want to remark that using Eq. (49) we get

$$\langle x^2(\tau,t')\rangle \simeq \begin{cases} C_1\frac{2(1-\alpha)}{\Gamma(3)}\tau^2 & \text{for } \tau \gg t' \gg T, \\ C_2\frac{2(1-\alpha)}{\Gamma(\alpha)\Gamma(4-\alpha)}\frac{\tau^{3-\alpha}}{t'^{(1-\alpha)}} & \text{for } T \ll \tau \ll t', \end{cases} \tag{59}$$

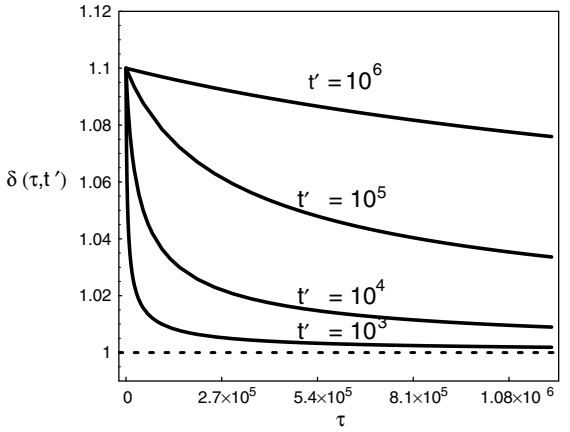

Fig. 7. Plotted the analytical scale dependence on forward time(τ) Eq. (56) for four different observation times: $t' = 10^3,\ 10^4,\ 10^5,\ 10^6$; $\mu = 1.8$.

an important result that proves that in the condition (a) the ballistic scaling applies, and in condition (b), in accordance with the results of Section 4, the scaling of Eq. (17) holds true. In Eq. (59) C_1 and C_2 are time independent constants and $\Gamma(z)$ is the Euler gamma function.

6. From a single trajectory to diffusion

There is one problem left to solve. This is the explanation of why the SDA reveals only the brand new scaling and is insensitive to the condition (b). To solve this remaining problem we have to address the important issue of how to turn a single sequence into a Gibbs ensemble. As mentioned in Section 1, a diffusion trajectory running for a time l is obtained by locating a window of size l at a given distance from the origin. Let us assume for simplicity that an event occurs at the origin of the sequence. Then we might be tempted to define the age of the window as the distance from the origin. In this case for any age we would obtain only one window, and as a consequence we cannot use this criterion.

Also the authors of Ref. [22] addressed the problem of deriving from a single sequence a Gibbs ensemble of age t'. Their method rests on setting the observation beginning at a distance t' from each event of the sequence under study. This criterion was proved to be efficient and accurate to assess the renewal nature of the single sequence under study. Unfortunately, it cannot be applied in the present case. In fact, it would lead to the absurd result that a single window of length l, to use for the creation of a diffusional trajectory with the same length, would have different ages, because the events on the left-hand side of this window have different distances from its left border. Therefore we have decided to define as age of a given diffusion trajectory of length l the distance between its beginning and the closest of the earlier events. As a consequence of this assumption the distribution density of the first event occurring, at a fixed age t', is given by

$$\psi(\tau, t') = (\mu - 1)\frac{(t' + T)^{\mu-1}}{(\tau + t' + T)^{\mu}}. \tag{60}$$

By repeating the treatment of Section 5 with this definition of $\psi(\tau, t')$, we obtain for the second moment, in the limiting case $\tau \gg T$, the following result

$$\langle x^2(\tau, t')\rangle \cong (T + \tau + t')^{\alpha+1}\left[\frac{2(T + \tau + t')^2 + \alpha^2\tau^2}{2 - \alpha} - \frac{\alpha\tau(2T + 3\tau + 2t')}{2 - \alpha}\right] - \frac{2(T + t')^{\alpha}(T + \tau + t')^3}{2 - \alpha}. \tag{61}$$

Of course, in this case the symbol $\langle\cdots\rangle$ indicates an average over the windows of the same age t'.

For the scaling $\delta(\tau, t')$ we obtain

$$\delta(\tau, t') \cong (2 - \alpha)\tau\left[\frac{(T + t')^{\alpha}(T + \tau + t')}{C(\tau, t') - D(\tau, t')} - \frac{(T + \tau + t')^{\alpha}(T + (1 - \alpha)\tau + t')}{C(\tau, t') - D(\tau, t')}\right], \tag{62}$$

where

$$C(\tau,t') \equiv 2(T+t')^{\alpha}(T+\tau+t')^{2} \tag{63}$$

and

$$D(\tau,t') \equiv (T+\tau+t')^{\alpha}[\alpha^{2}\tau^{2}+2(T+\tau+t')^{2}-\alpha\tau(2T+3\tau+2t')]. \tag{64}$$

In the time asymptotic limit we obtain

$$\delta(\tau,t') \cong \begin{cases} \frac{3}{2} & \text{for } T \ll \tau \ll t', \\ 1 & \text{for } T \ll t' \ll \tau. \end{cases} \tag{65}$$

So, for the infinitely aged and the brand new condition we have $\delta = \frac{3}{2}$ and $\delta = 1$, respectively.

We have to explain why the SDA is insensitive to the infinitely aged scaling, which is, by the way different from the infinitely aged scaling of Eq. (17) emerging from the average over the systems of a genuine Gibbs ensemble (see Section 5). It is evident that the statistical weight of condition (b) is much smaller than that of condition (a), thereby explaining why the statistical analysis of Section 2 does not reveal it. Let us see why it is so. We have to define the statistical weight $W(t')$. We use the following formula

$$W(t') = N\Psi(t'), \tag{66}$$

where

$$\Psi(t') = \int_{t'}^{+\infty} \psi(\tau)\,\mathrm{d}\tau = \left(\frac{T}{t'+T}\right)^{\mu-1}. \tag{67}$$

The explanation of this choice is as follows. As we increase the distance between the left border of the mobile window and a given event, the probability of meeting a new event increases. When a new event is found, we reset to zero the window's age. Thus, the statistical weight of a given distance t' from an earlier event is proportional to the survival probability $\Psi(t')$. In the case $\mu < 2$ this weight cannot be normalized. However, we have to take into account that the sequence under study is finite. Therefore the age t' cannot exceed a maximum value $\tau_{\max}$. This makes it possible for us to set

$$\int_{0}^{\tau_{\max}} W(t')\,\mathrm{d}t' = 1, \tag{68}$$

which defines the normalization constant N and allows us to write

$$W(t') = \frac{(2-\mu)}{[(T+\tau_{\max})^{2-\mu} - T^{2-\mu}]} \cdot \frac{1}{[T+t']^{\mu-1}}. \tag{69}$$

In Figs. 8 and 9 we illustrate the form of the statistical weight $W(t')$. The weight $\Pi(\delta)$ of the aging dependent scaling $\delta(t')$ is defined by means of

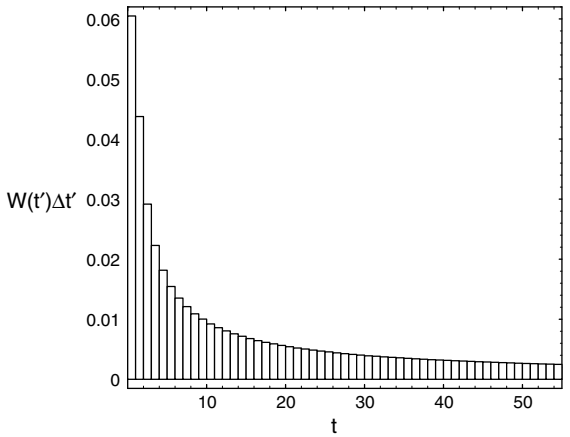

Fig. 8. Numerical statistical weight ($W[t']$) for a single sequence length $L_{\max} \simeq 4.3 \times 10^{6}$ and maximum event time $\tau_{\max} \simeq 9.92 \times 10^{5}$. $\mu = 1.8,\ \Delta t' = 1,\ T = 1$.

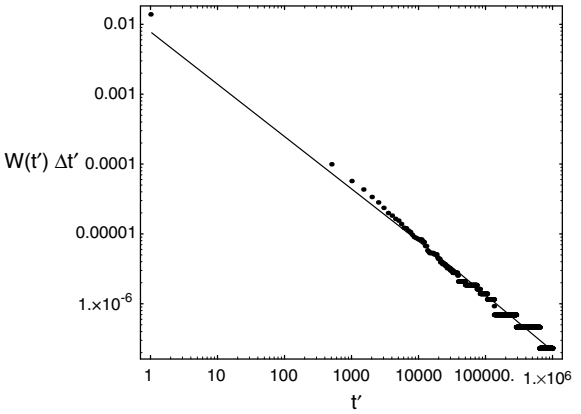

Fig. 9. Similar as in Fig. 8. The solid line is analytical, Eq. (69), and the dots are numerical $W(t')$ weight. Both in log–log scale. The numerical constants are: $\mu = 1.8,\ T = 1,\ \Delta t' = 1$, the total sequence length $\equiv L_{\max} \simeq 4.3 \times 10^6,\ \tau_{\max} \simeq 9.92 \times 10^5$.

$$\Pi(\delta)\,\mathrm{d}\delta = W(t')\,\mathrm{d}t'. \tag{70}$$

To do the numerical calculation, we operate as follows. We consider a sequence of length $L < L_{\max}$. The statistical weight of δ is determined by

$$\Pi[\delta, L] = W[t'(\delta, L)]\left|\frac{\partial t'(\delta, L)}{\partial \delta}\right|. \tag{71}$$

The function $t'(\delta, L)$ is obtained in the following way. We move t' from $+0$ to $\tau_{\max}$ so as to find $\delta(L, 0)$ and $\delta(L, \tau_{\max})$ for a fixed L. Due to the monotonic dependence of $\delta(L, t')$ on t' we find

$$t' = t'(\delta, L), \tag{72}$$

which is well defined function of δ for δ running from $\delta(L, 0)$ to $\delta(L, \tau_{\max})$. The function of Eq. (72) is obtained numerically with a very good accuracy. Finally, we plot the function $\Pi(\delta, L)$ for a given L and $0 \leqslant t' \leqslant \tau_{\max}$, which is shown in Fig. 10. In Fig. 10 the left and right peaks correspond to $t' \ll L$ and $t' \gg L$, or to the so called brand new and largely aged scaling, respectively. Then we evaluate the average of δ defined by

$$\langle\delta\rangle_L \equiv \int_0^{\tau_{\max}} W(t')\delta(L, t')\,\mathrm{d}t'. \tag{73}$$

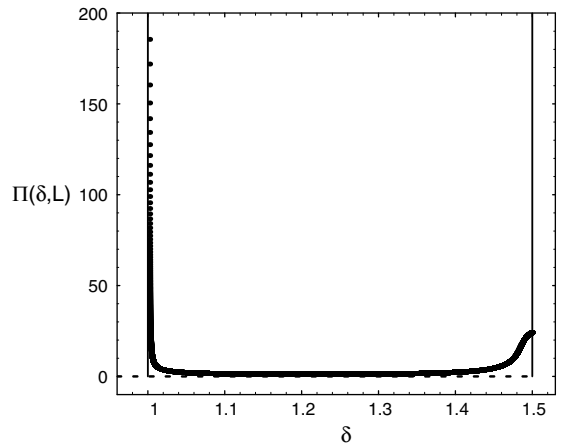

Fig. 10. The numerical plot of the weight of the scale Eq. (71), for a given window length $\equiv L = 10^3;\ 0 \leqslant t' \leqslant 10^4,\ \mu = 1.8,\ T = 1$, sequence length $\equiv L_{\max} = 10^5$.

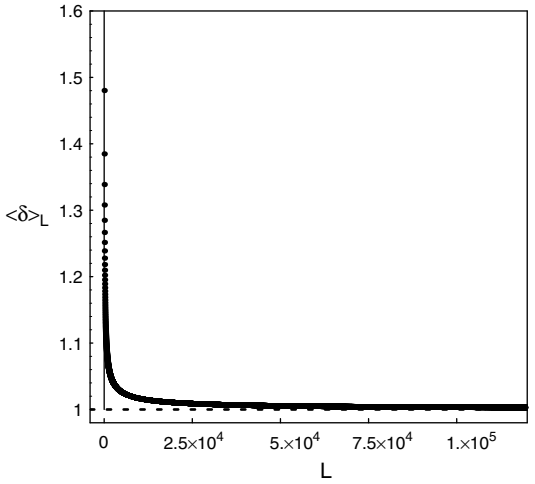

Fig. 11. The plot of average scale vs. window length, $\langle\delta\rangle_L \equiv \langle\delta(L)\rangle$. That is it is plotted the numerically integrated form of Eq. (73) for the following constants: $\mu = 1.8,\ \tau_{\max} = 10^2,\ T = 1,\ L_{\max} = 10^5$ (total length of the sequence).

Note that the mobile windows must have size very small compared to the size of the whole sequence length($L_{\max}$) so as to produce enough statistics from a finite sequence. Fig. 11 shows that the the mean value of δ drops very quickly to the ballistic prescription $\delta = 1$, thereby explaining why the SDA is insensitive to the aging effects.

7. Concluding remarks

The main results of this paper can be summarized as follows. The non-ergodic condition $\mu < 2$ generates aging, and consequently an aging dependent scaling. If we adopt the Gibbs perspective the dependence of scaling on aging can be established adopting rigorous prescriptions of the literature on renewal processes. The SDA, DEA and DFA are methods developed to analyze single sequences, thereby making it necessary to use a time average rather than an ensemble average. In the case $\mu > 2$ this is not a problem, insofar as the ergodic condition is fulfilled. Previous work [4,15] showed that, while SDA and DFA estimate the scaling of the diffusion pdf variance, DEA directly estimates the scaling of the pdf (Eq. 3), which in the Lévy case is different from the variance scaling.

In the case $\mu < 2$, the correspondence between the two averaging ways is not guaranteed anymore. The theoretical investigation done in Section 5 shows that two scalings are admitted, the aged scaling, $\delta = (4 - \mu)/2$, and the brand new scaling $\delta = 1$. The emergence of $\delta > 1$ is therefore not a numerical artifact, and is not a violation of the physical constraint of keeping $\delta \leqslant 1$, either. The analysis of Section 5 although based on the second moment shows that this scaling has a clear physical meaning and corresponds to the aged condition. This result offers an explanation of the DFA scaling $\delta = (4 - \mu)/2$, not affected by the transition from the ergodic to the non-ergodic regime, as caused by the predominance of the aged condition. We argue that this is an effect of the detrending process built in the DFA analysis, and urge for further investigations to support this point. As far as the SDA is concerned, the analysis done in Section 6 explains the SDA scaling $\delta = 1$ by showing that SDA estimate is based on windows which are mostly in the brand new condition, causing the influence of the aged condition to be marginal. The DEA probably tends asymptotically to the same scaling as the DFA. If it does, it is however remarkable that the DFA keeps a connection with the aged condition, with extremely good accuracy, for the whole time observation range. This result offers a physical interpretation of the DFA scaling exponent estimated from non-ergodic time series, giving a theoretical support to many interdisciplinary investigations that used this method in the non-ergodic regime [10–12].

Acknowledgment

We thankfully acknowledge ARO for the financial support of this research through grant # W911NF-05-1-0059.

References

[1] Peng C-K, Buldyrev SV, Havlin S, Simons M, Stanley HE, Goldberger AL. Phys Rev E 1994;49:1685.
[2] Grigolini P, Palatella L, Raffaelli G. Fractals 2001;9:439.
[3] Allegrini P, Barbi M, Grigolini P, West BJ. Phys Rev E 1995;52:5281.
[4] Scafetta N, Grigolini P. Phys Rev E 2002;66:036130.
[5] Allegrini P, Benci V, Grigolini P, Hamilton P, Ignaccolo M, Menconi G, et al. Chaos, Solitons & Fractals 2003;15:517.
[6] Taqqu SM, Teverovsky V, Willinger W. Fractals 1995;3:785.
[7] Lutz E. Phys Rev Lett 2004;97:190602.
[8] Margolin G, Barkai E. Phys Rev Lett 2005;94:080601.
[9] Bel G, Barkai E. Phys Rev Lett 2005;94:240602.
[10] Peng C-K, Havlin S, Stanley HE, Goldberger AL. Chaos 1995;5:82.
[11] Watters PA. Complexity 1998;5:1.
[12] Buiatti M, Papo D, Baudonniere PM, Van Vreeswijk C. Neuroscience, in press.
[13] Zumofen G, Klafter J. Phys Rev E 1993;47:851.
[14] Trefán G, Floriani E, West BJ, Grigolini P. Phys Rev E 1994;50:2564.
[15] Allegrini P, Bellazzini J, Bramanti G, Ignaccolo M, Grigolini P, Yang J. Phys Rev E 2002;66:015101 (R).
[16] Aquino G, Bologna M, Grigolini P, West BJ. Phys Rev E 2004;70:036105.
[17] Allegrini P, Aquino G, Grigolini P, Palatella L, Rosa A, West BJ. Phys Rev E 2005;71:066109.
[18] Buiatti M, Grigolini P, Palatella L. Physica A 1999;268:214.
[19] Scafetta N, Latora V, Grigolini P. Phys Rev E 2002;66:031906.
[20] Allegrini P, Barbi M, Grigolini P, West BJ. Phys Rev 1995;52:5281.
[21] Godréche G, Luck JM. J Stat Phys 2001;104:489.
[22] Bianco S, Grigolini P, Paradisi P. J Chem Phys 2005;123:174704.